World Academy of Science, Engineering and Technology
International Journal of Chemical and Molecular Engineering
Vol:10, No:12, 2016

Further Investigation of $\alpha+^{12}C$ and $\alpha+^{16}O$ Elastic Scattering

Sh. Hamada

***Abstract*—**The current work aims to study the rainbow like-structure observed in the elastic scattering of alpha particles on both ^{12}C and ^{16}O nuclei. We reanalyzed the experimental elastic scattering angular distributions data for $\alpha+^{12}C$ and $\alpha+^{16}O$ nuclear systems at different energies using both optical model and double folding potential of different interaction models such as: CDM3Y1, DDM3Y1, CDM3Y6 and BDM3Y1. Potential created by BDM3Y1 interaction model has the shallowest depth which reflects the necessity to use higher renormalization factor (N_r). Both optical model and double folding potential of different interaction models fairly reproduce the experimental data.

***Keywords*—**Nuclear rainbow, elastic scattering, optical model, double folding, density distribution

***PACS number(s)*—**21.60.Gx, 24.10.Ht.

I. Introduction

STUDY of nuclear interactions is of special interest as it could provide us with useful information about nuclear structure and mechanism of interaction. One of the most interesting features which could be observed in study of nuclear reactions is nuclear rainbow phenomenon. This phenomenon was first realized in the scattering of alpha particles [1]. Similar effects were seen in the scattering of the light heavy ions ^{6}Li [2], [3], in the elastic scattering of some nuclear system such as $^{16}O+^{12}C$ [4]-[6], $^{12}C+^{12}C$ [7]-[12], $^{16}O+^{16}O$ [13], [14] and also in ^{3}He and α-nucleus elastic and inelastic scattering [15]-[18]. The elastic scattering angular distributions for these nuclear systems reveal refractive features, such as rainbow scattering patterns and broad interference minima ''Airy minima'' [19]. Nuclei are well known to have wave properties and they may suffer from being diffracted, refracted and also from interference. Consequently, the nucleus-nucleus scattering may display rainbow features depending on: The scattering conditions, energy of the incident projectile and the binding structure of the projectile and target. The rainbow could be observed well in the elastic scattering whereas there is no change in the total flux. Therefore, the nuclear rainbow should be strongest in the elastic scattering channel especially in nuclear systems with small absorption.

In the present work, we reanalyzed both $\alpha+^{12}C$ and $\alpha+^{16}O$ elastic scattering angular distributions using both optical model (OM) and double folding potential (DFP) of different interaction models such as: CDM3Y1, DDM3Y1, CDM3Y6 and BDM3Y1. All these different interaction models are essentially based on the basic form of M3Y Reid or M3Y Paris, but the main difference between them lies in the values of the parameters used in calculating density dependent function $F(\rho)$. We have extracted the renormalization factor (N_r) for ($\alpha+^{12}C$ and $\alpha+^{16}O$) nuclear systems at the different concerned energies within the framework of the different concerned interaction models.

In the previous studies for $\alpha+^{16}O$, Michel et al. [20] presented a systematic OM analysis for $^{16}O(\alpha,\alpha)^{16}O$ elastic scattering with a new parametrization for the real part of the potential, whereas for the imaginary part they used a squared Woods-Saxon form factor. The extracted potential in Michel's work gives a precise description of $\alpha+^{16}O$ elastic scattering data in the energy range between 30 and 150 MeV. H. Abele et al. [21] analyzed $\alpha+^{16}O$ elastic scattering data using an early version for DFP and the renormalization factor allowed to be varied from 1.395 at the lowest energy down to 1.275 at the highest energy. M. El-Azab Farid [15] used the single folding cluster (SFC) [22] and double folding cluster (DFC) [23], [24] models to analyze the experimental data for $\alpha+^{16}O$ elastic scattering and he obtained a reasonable fitting. H. Abele et al. [21] analyzed the $\alpha+^{12}C$ elastic scattering, the real part of the potential was calculated using DFP with DDM3Y model of *NN* interaction and the imaginary potential was expressed in terms of a Fourier-Bessel function of six terms. Khallaf et al. [25] analyzed this nuclear system using the JLM *NN* interaction.

In the current work, we tried to analyze $\alpha+^{12}C$ and $\alpha+^{16}O$ elastic scattering data using OM and DFP of different models of interaction and to extract N_r from the different concerned interaction models. Based on the theoretical calculation, rainbow phenomenon and Airy minima are well reproduced and presented.

The rest of the paper is organized as follows. In Section II the theoretical analysis of the experimental data is presented and Section III is devoted to the results and discussion. The summary is given in Section IV.

II. Theoretical Analysis

A. Elastic Scattering in the Framework of OM

The elastic scattering angular distributions for both $\alpha+^{12}C$ and $\alpha+^{16}O$ are firstly reanalyzed within the framework of the standard OM of the nucleus. The interaction potential could be written as:

Sh. Hamada is with Faculty of Science, Tanta University, Tanta, Egypt (e-mail: sh.m.hamada@science.tanta.edu.eg).

$$U(r) = V_C - V_0\left[1+\exp\left(\frac{r-R_V}{a_V}\right)\right]^{-1} - iW_0\left[1+\exp\left(\frac{r-R_W}{a_W}\right)\right]^{-1} \quad (1)$$

with radius:

$$R_i = r_i(A_T^{1/3}),\ i = V, W, C$$

This potential consists of three parts: a- Real volume part, b- Imaginary volume part and c- Coulomb potential of a uniform charged sphere. Real and imaginary parts of the potential are taken to be of Woods-Saxon form factor.

In OM calculations, the differential cross section could be easily calculated as the square of scattering amplitude $\frac{d\sigma}{d\Omega} = |f(\theta,\varphi)|^2$, and the elastic nucleus-nucleus scattering amplitude can be expressed in the form:

$$f(\theta) = f_c(\theta) + \frac{i}{2k}\sum_l (2l+1)\exp(2i\sigma_l)(1-S_l)P_l(\cos\theta) \quad (2)$$

where $f_c(\theta)$ is the amplitude of the Coulomb scattering, σ_l is the Coulomb phase shift, k is the wave number, S_l is the scattering matrix element for the l-th partial wave, and $P_l(\cos\theta)$ is the Legendre polynomial.

It is frequently found that many sets of parameters give good fits to the data, and the question then arises whether any one of these sets is more physical than the others, and if so which is to be preferred. These parameter ambiguities are of two main types, discrete and continuous. Discrete ambiguities refer to regions of parameter space that give acceptable fits separated by unacceptable regions. Continuous ambiguities refer to combinations of parameters that may be simultaneously varied being subjected to some constraint without significantly affecting the fit. The existence of these and other more complicated parameter ambiguities means that it is not possible to establish the optical potential (OP) by phenomenological analyses alone. It is necessary to start by constraining the potential as closely as possible by physical requirements before parameter optimization. So, it is preferable to use more microscopic potential such as folding potential.

B. Elastic Scattering in the Framework of Double Folding

The DFP for $\alpha+^{12}C$ and $\alpha+^{16}O$ at the different concerned energies are prepared using code DFMSPH [26]. In the double folding (DF) calculations, the real part of the potential is calculated from a more fundamental basis by the DF method in which the nucleon-nucleon interaction potential is folded into the densities of both the projectile and target nuclei:

$$V^{DF}(\vec{R}) = \iint \rho_p(\vec{r}_1)\rho_t(\vec{r}_2)V_{NN}\left(\left|\vec{R}+\vec{r}_2-\vec{r}_1\right|\right)d^3\vec{r}_1 d^3\vec{r}_2 \quad (3)$$

where $\rho_p(\vec{r}_1)$ and $\rho_t(\vec{r}_2)$ are the nuclear matter density distributions of both the projectile and target nuclei respectively, and $V_{NN}(|\vec{R}+\vec{r}_2-\vec{r}_1|)$ is the effective NN interaction potential which gives the corresponding values of the nuclear incompressibility K in the Hartree-Fock (HF) calculation of nuclear matter and it was taken to be of the CDM3Y1 and CDM3Y6 form based on the M3Y-Paris potential:

$$v_D(s) = 11061.625\frac{\exp(-4s)}{4s} - 2537.5\frac{\exp(-2.5s)}{2.5s},$$
$$v_{EX}(s) = -1524.25\frac{\exp(-4s)}{4s} - 518.75\frac{\exp(-2.5s)}{2.5s} - 7.8474\frac{\exp(-0.7072s)}{0.7072s} \quad (4)$$

and also BDM3Y1 and DDM3Y1 form based on the M3Y-Reid potential:

$$v_D(s) = 7999.0\frac{\exp(-4s)}{4s} - 2134.25\frac{\exp(-2.5s)}{2.5s},$$
$$v_{EX}(s) = -4631.38\frac{\exp(-4s)}{4s} - 1787.13\frac{\exp(-2.5s)}{2.5s} - 7.8474\frac{\exp(-0.7072s)}{0.7072s} \quad (5)$$

The M3Y-Paris and M3Y- Reid interactions are scaled by an explicit density-dependent function $F(\rho)$:

$$v_{D(EX)}(\rho,s) = F(\rho)v_{D(EX)}(s), \qquad S = \left|\vec{R}+\vec{r}_2-\vec{r}_1\right| \quad (6)$$

v_D and v_{EX} are the direct and exchange components of the M3Y-Paris and M3Y- Reid, ρ is the nuclear matter density. The density-dependent function is expressed as:

$$F(\rho) = C[1+\alpha\exp(-\beta\rho) - \gamma\rho^n], \quad (7)$$

The parameters C, α, β, γ, n for the different concerned interaction models listed in Table I were taken from [27],

TABLE I
PARAMETERS OF DENSITY DEPENDENCE FUNCTION $F(\rho)$

Interaction Model	C	α	β (fm^3)	γ (fm^{3n})	n	K (MeV)
CDM3Y6	0.2658	3.8033	1.4099	4.0	1	252
CDM3Y1	0.3429	3.0232	3.5512	0.5	1	188
BDM3Y1	1.2253	0.0	0.0	1.5124	1	232
DDM3Y1	0.2845	3.6391	2.9605	0.0	0	171

The density distributions of α, ^{12}C and ^{16}O are expressed in a modified form of the Gaussian shape as: $\rho(r) = \rho_0(1+wr^2)\exp(-\beta r^2)$, the parameters ($\rho_0$, w, β) for α-particles, ^{12}C and ^{16}O are listed in Table II.

III. Results and Discussion

A. $\alpha+^{12}C$ Nuclear System

Both the phenomenological (OM) and semi microscopic (DF) calculations are performed using code FRESCO and code SFRESCO [30]. The comparisons between the

experimental data for $\alpha+^{12}C$ nuclear system at energies (104, 120, 139, 145, 166 and 172.5 MeV) [31]-[35] and the theoretical calculations within the framework of OM are shown in Fig. 1. The radius parameter for real volume part of potential (r_V) was fixed at 1.245 fm, radius parameter for the imaginary volume part of potential (r_W) was fixed at 1.6 fm, and radius parameter for the Coulomb part of potential (r_C) was fixed at 1.25 fm. The optimal OP parameters are listed in Table II.

Nearside and farside components of cross sections are calculated using the same the potential parameters listed in Table II. As shown in Fig. 1, the most significant contribution for the cross section comes from the farside component. The farside components at energies 104, 120, 139, 145, 166 and 172.5 MeV predicted the position of Airy minimum to be around 24.8°, 23.7°, 23.2°, 21.3°, 20.9° and 19.8° respectively. The significant increase in cross section at backward angles at energy 104 MeV might indicate that other non-scattering events, like the elastic alpha cluster transfer process, still contribute to the elastic cross section at this energy.

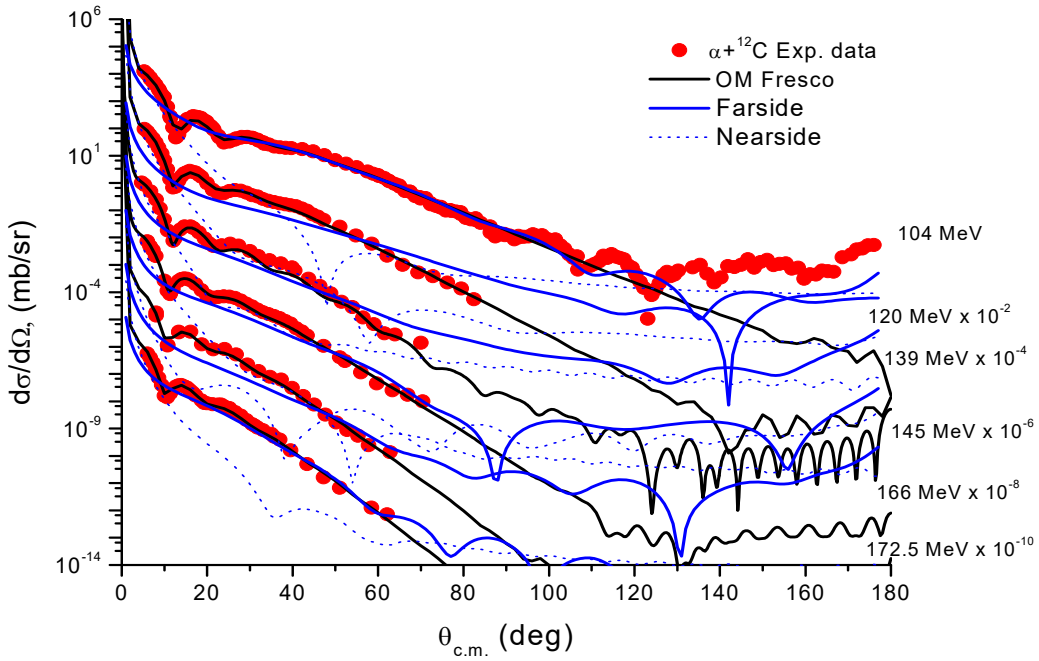

Fig. 1 The comparison between the experimental data for $\alpha+^{12}C$ elastic scattering at energies (104, 120, 139, 145, 166 and 172.5 MeV) and the theoretical calculations using OM

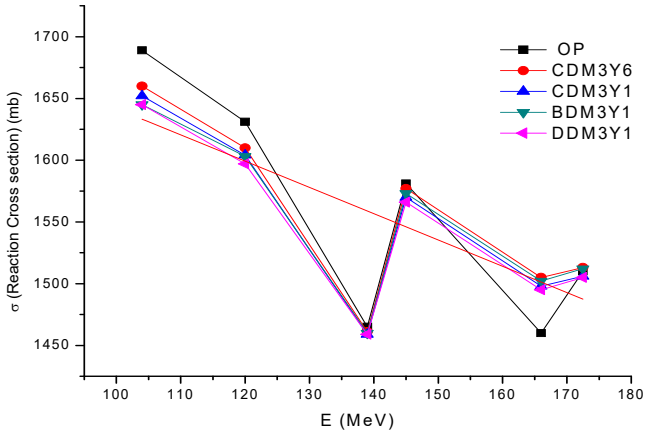

Fig. 2 The variation of reaction cross section with energy

We have calculated the reaction cross section (σ_R) for $\alpha+^{12}C$ nuclear system at the different concerned energies using both OM and DFP of different interaction models as shown in Fig. 2. The energy dependence of reaction cross section can be expressed as: $\sigma = 1854 - 2.128\ E$.

The quality of the fitting of OM and DF calculations to the experimental data can be estimated using the χ^2 - method, which is represented as:

$$\chi^2 = \frac{1}{N}\sum_{i=1}^{N}\left[\frac{\sigma_i^t(\theta)-\sigma_i^e(\theta)}{\Delta\sigma_i^e(\theta)}\right]^2 = \frac{1}{N}\sum_{i=1}^{N}\chi_i^2 \qquad (8)$$

where σ^e and σ^t are the experimental and theoretical differential cross sections of the elastic scattering for i-th scattering angle, $\Delta\sigma^e$ is the error of the experimental differential cross sections at these angles, N is the number of measurements. χ^2/N values are listed in Table II, the less the value χ^2 is, the better is the description of the experimental data in terms of the selected theoretical representation.

TABLE II
OP AND DF PARAMETERS FOR α-PARTICLES ELASTICALLY SCATTERED ON ^{12}C AT DIFFERENT ENERGIES

E (MeV)	Model	V_o (MeV)	a_v (fm)	W_o (MeV)	a_w (fm)	N_r	σ_R (mb)	Jv (MeV.fm^3)	Jw (MeV.fm^3)	χ^2/N
172.5	OM	90.38	0.772	22.02	0.663		1510	315.4	125	3.02
	DF- CDM3Y1			22.02	0.663	1.111	1506	287.5	125	1.74
	DF- DDM3Y1			22.02	0.663	1.166	1505	282.0	125	1.51
	DF- CDM3Y6			22.02	0.663	1.181	1513	287.38	125	1.54
	DF- BDM3Y1			22.02	0.663	1.238	1512	268.56	125	1.51
166	OM	90.43	0.745	21.29	0.6347		1460	306.38	118.38	16.11
	DF- CDM3Y1			21.29	0.6347	1.118	1498	305.08	118.38	10.28
	DF- DDM3Y1			21.29	0.6347	1.172	1495	285.94	118.38	8.97
	DF- CDM3Y6			21.29	0.6347	1.1804	1505	290.8	118.38	9.97
	DF- BDM3Y1			21.29	0.6347	1.236	1502	272.7	118.38	9.99
145	OM	92.77	0.772	21.14	0.69		1581	323.7	122.4	4.16
	DF- CDM3Y1			21.14	0.69	1.0827	1570	317.6	122.4	2.32
	DF- DDM3Y1			21.14	0.69	1.1352	1566	300.28	122.4	2.43
	DF- CDM3Y6			21.14	0.69	1.137	1577	303.02	122.4	2.25
	DF- BDM3Y1			21.14	0.69	1.191	1573	286.6	122.4	2.45
139	OM	93.65	0.712	25.68	0.626		1465	306.1	129.8	2.89
	DF- CDM3Y1			25.68	0.493	1.041	1459	321.5	129.8	6.62
	DF- DDM3Y1			25.68	0.493	1.08	1459	304.56	129.8	6.64
	DF- CDM3Y6			25.68	0.493	1.099	1461	306.6	129.8	7.05
	DF- BDM3Y1			25.68	0.493	1.1366	1460	290.73	129.8	7.24
120	OM	96.12	0.772	20.98	0.673		1631	335.4	119.9	3.39
	DF- CDM3Y1			20.98	0.673	1.0574	1604	333.56	119.9	2.39
	DF- DDM3Y1			20.98	0.673	1.0917	1597	318.44	119.9	2.96
	DF- CDM3Y6			20.98	0.673	1.1068	1610	318.21	119.9	2.58
	DF- BDM3Y1			20.98	0.673	1.1413	1603	304.17	119.9	3.21
104	OM	100.6	0.769	19.55	0.694		1689	349.9	113.5	2.72
	DF- CDM3Y1			19.55	0.694	1.0645	1652	344.08	113.5	2.44
	DF- DDM3Y1			19.55	0.694	1.0976	1645	330.7	113.5	2.45
	DF- CDM3Y6			19.55	0.694	1.1193	1660	328.34	113.5	2.43
	DF- BDM3Y1			19.55	0.694	1.1413	1645	315.98	113.5	1.38

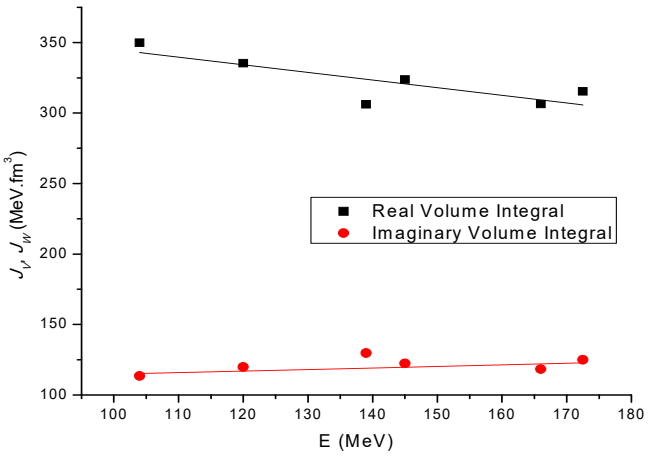

Fig. 3 Energy dependence of real (Jv) and imaginary (Jw) volume integral

OP and DFP can conveniently be characterized by the real and imaginary volume integrals per nucleon:

$$Jv = -\frac{4\pi}{A_P A_t}\int_0^\infty V(r)r^2dr, \quad J_w = -\frac{4\pi}{A_P A_t}\int_0^\infty W(r)r^2dr \qquad (9)$$

The J_v values in our work ranged between 268.56 and 335.4 MeV.fm^3 and J_w between 113.5 and 129.8 MeV.fm^3 as listed in Table II which agree well with the previously existing theoretical estimations [15]. The energy dependence of real volume integral in this work could be expressed as J_v = 399.5-0.543E, and for imaginary volume integral J_w = 103.84+0.109E as shown in Fig. 3.

The dependence of V_0 and W_0 values for $^{12}C(\alpha, \alpha)^{12}C$ on energy are shown in Figs. 4 (a) and (b) and can be approximated by:

(a) V = 113.9-0.14E,

(b) W = 17.16+0.027E.

The comparison between the experimental data for $\alpha+^{12}C$ at energies (104, 120, 139, 145, 166 and 172.5 MeV) and the DF calculations of different interaction models: CDM3Y1, DDM3Y1, CDM3Y6 and BDM3Y1 are shown in Figs. 5, 6, 7 and 8 respectively. Optimal potential parameters for $\alpha+^{12}C$ nuclear system, also those from DF of different interaction models are listed in Table II. The obtained renormalization factor (N_r) for $\alpha+^{12}C$ nuclear system is in the range 1.041-1.238. The optimal parameters for the imaginary part of potential obtained from OM were kept constant during the DF calculations. The interaction potential in this case has the shape:

$$U(R) = V_C + Nr\,V^{DF}(R) - iW(R) \qquad (10)$$

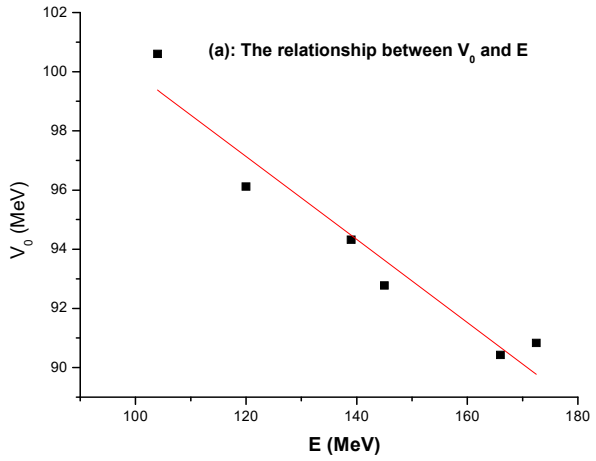

Fig. 4 (a) The relationship between real potential depth and energy

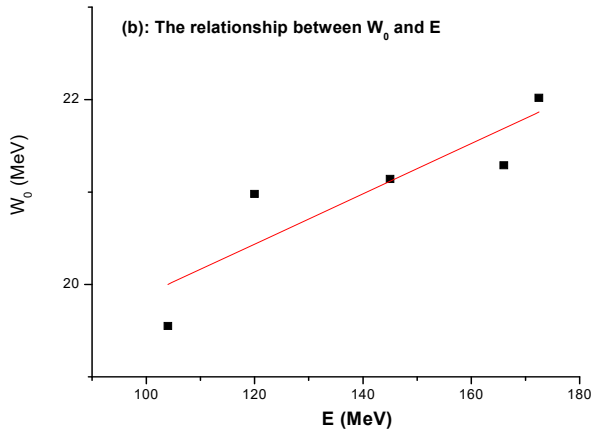

Fig. 4 (b) The relationship between imaginary potential depth and energy

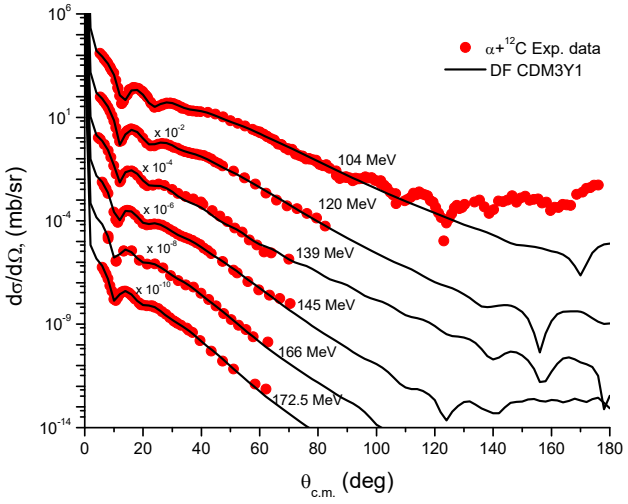

Fig. 5 The comparison between the experimental data for $\alpha+^{12}C$ at energies (104, 120, 139, 145, 166 and 172.5 MeV) and the theoretical calculations using DFP of interaction model CDM3Y1

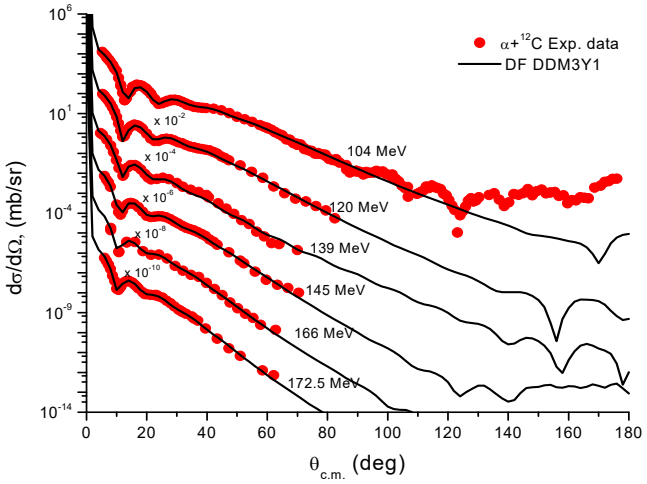

Fig. 6 The same as Fig. 5 but for interaction model DDM3Y1

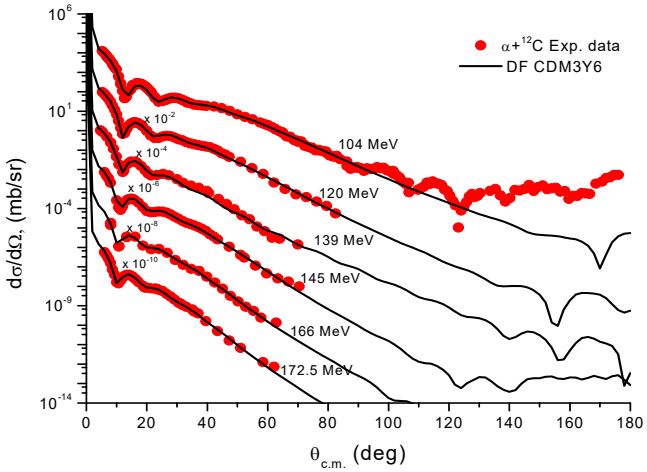

Fig. 7 The same as Fig. 5 but for interaction model CDM3Y6

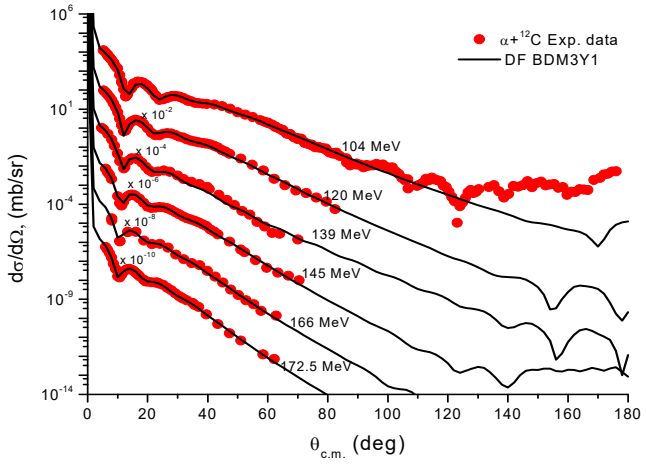

Fig. 8 The same as Fig. 5 but for interaction model BDM3Y1

The Airy minimum could be observed for $^{12}C(\alpha,\alpha)^{12}C$ elastic scattering at the aforementioned energies. The characteristic features of the falloff of the cross section beyond the rainbow angle in the experimental angular distributions are

well reproduced. As shown in Fig. 1, with increasing the energy of the incident projectile, the position of rainbow angle is shifted toward small angles. The angular position of rainbow angle at the different concerned energies is shown in Fig. 9.

As we discussed before, the calculations in this work are performed using different four models of interaction: CDM3Y1, DDM3Y1, CDM3Y6 and BDM3Y1. The used DFP consists of two parts direct part and exchange part. Fig. 10 shows the variation of the potential depth with radius for the direct and exchange parts of the potential and also their sum (direct + exchange) at E=172.5 MeV, this figure also shows variation of the potential depth with radius at the different concerned alpha particles energies. Fig. 11 shows how the potential is created by BDM3Y1 model of interaction is shallower in comparison with the rest which reflect the necessity to use higher renormalization factor.

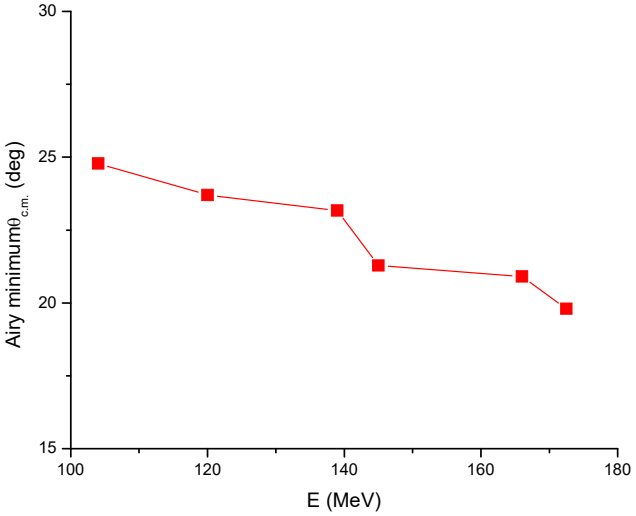

Fig. 9 Angular position of the Airy minimum for $\alpha+^{12}C$ elastic scattering at energies 104, 120, 139, 145, 166 and 172.5 MeV. The lines are only to guide the eye

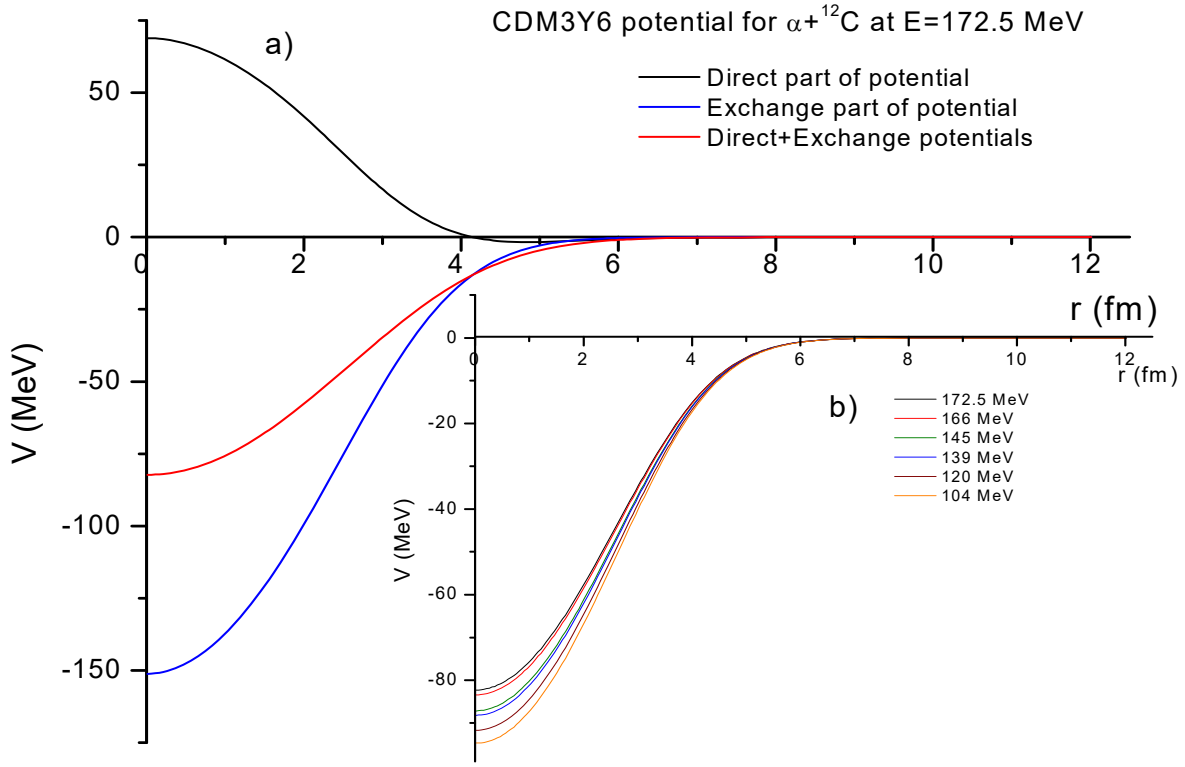

Fig. 10 (a) The variation of the potential depth with radius for both direct and exchange parts of the potential and also their sum (direct + exchange) at E=172.5 MeV; (b) the variation of the potential depth with radius at different energies

B. $\alpha+^{16}O$ Nuclear System

The comparison between the experimental data for $\alpha+^{16}O$ nuclear system at energies 49.5, 69.5, 80.7 and 104 MeV [20], [33], [36] and the theoretical calculations within the framework of OM is shown in Fig. 12. The radius parameter for real volume part of potential (r_V) was fixed at 1.36 fm, radius parameter for imaginary volume part of potential (r_W) was fixed at 1.73 fm and radius parameter for the Coulomb part of potential (r_C) was fixed at 1.25 fm.

The comparisons between the experimental data for $\alpha+^{16}O$ at energies 49.5, 69.5, 80.7 and 104 MeV and the DF calculations of different interaction models: CDM3Y1, DDM3Y1, CDM3Y6 and BDM3Y1 are shown in Figs. 13, 14, 15 and 16 respectively. Optimal OP parameters for $\alpha+^{16}O$ nuclear system, also those from DF of different interaction models are listed in Table III. The obtained N_r for $\alpha+^{16}O$

nuclear system is in the range of 1.1157-1.3312. The imaginary part of the potential was taken in the form of standard Woods-Saxon form factor, the same optimal parameters for the imaginary part of potential obtained from OM calculations were kept constant during the DF calculations, and the used interaction potential has the same shape as in (10).

The nuclear rainbow phenomenon could be clearly observed in $^{16}O(\alpha,\alpha)^{16}O$ elastic scattering at the aforementioned energies. The characteristic features of the falloff of the cross section beyond the rainbow angle in the experimental angular distributions are well reproduced. Both OM and DF of different interaction models: CDM3Y1, DDM3Y1, CDM3Y6 and BDM3Y1 could reasonably reproduce the experimental data. The angular distribution data and the OM calculations at E= 49.5 MeV showed that the Airy minimum is ≈ 78°, but the DF calculations expected the minimum to be ≈ 75° and this may be due to the existence of a valley of two minima: the first minimum at 78° as shown in Fig. 12 and the second probably at 70° (not shown in the experimental data). DF calculations expected that the position of Airy minimum is ≈ 48° at E=69.5 MeV as shown in Figs. 13-16, while from the OM calculations it is around 40° as shown in Fig. 12, the minimum at ≈ 48° could not be observed from experimental data. At energies 80.7 and 104 MeV, both OM and DF calculations expected the same position for Airy minimum (35° at E=80.7 MeV and 31° at E=104 MeV). As shown in Figs. 12-16, with increasing the energy of the incident projectile, the position of rainbow angle is shifted toward small angles. The angular position of rainbow angle at the different concerned energies is shown in Fig. 17.

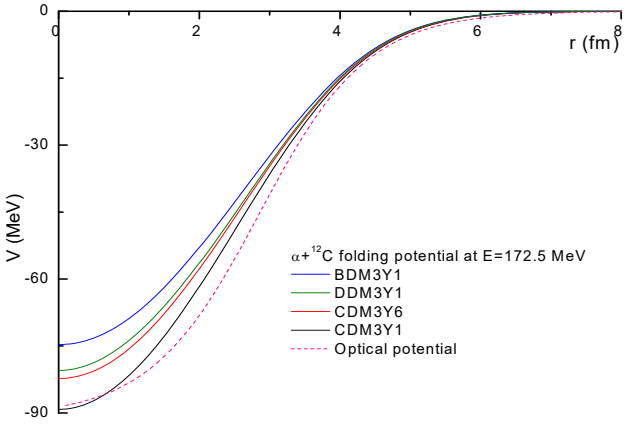

Fig. 11 The variation of the potential depth with radius for $\alpha+^{12}C$ DFP at E=172.5 MeV using different models of interaction BDM3Y1, DDM3Y1, CDM3Y6 and CDM3Y1 and also OP

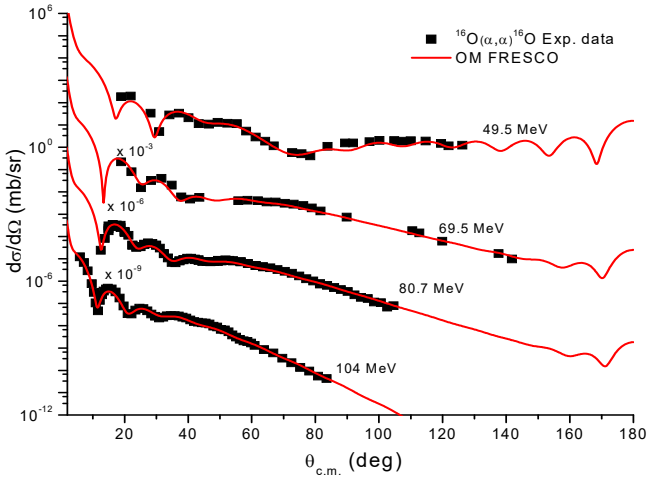

Fig. 12 The comparison between the experimental data for $\alpha+^{16}O$ at energies (49.5, 69.5, 80.7 and 104 MeV) and the theoretical calculations using OM

TABLE III
OP AND DF PARAMETERS FOR α-PARTICLES ELASTICALLY SCATTERED ON ^{16}O AT DIFFERENT ENERGIES

E (MeV)	Model	V_o (MeV)	a_v (fm)	W_o (MeV)	a_w (fm)	N_r	σ_R (mb)	Jv (MeV.fm^3)	Jw (MeV.fm^3)	χ^2/N
49.5	OM	109.63	0.6	8.94	0.739		1871	376.18	62.22	10.99
	DF- CDM3Y1			8.94	0.739	1.1228	1872	382.18	62.22	7.6
	DF- DDM3Y1			8.94	0.739	1.1474	1861	375.87	62.22	7.97
	DF- CDM3Y6			8.94	0.739	1.1931	1887	365.14	62.22	8.41
	DF- BDM3Y1			8.94	0.739	1.2143	1874	359.03	62.22	8.3
69.5	OM	99.99	0.715	15.58	0.648		2006	376.66	102.9	5.78
	DF- CDM3Y1			15.58	0.648	1.1209	1983	367.75	102.9	3.59
	DF- DDM3Y1			15.58	0.648	1.1458	1973	359.0	102.9	2.33
	DF- CDM3Y6			15.58	0.648	1.1782	1990	350.89	102.9	3.53
	DF- BDM3Y1			15.58	0.648	1.2002	1979	342.92	102.9	2.59
80.7	OM	101.26	0.714	16.7	0.556		1923	381.13	105.08	2.74
	DF- CDM3Y1			16.7	0.556	1.1307	1894	359.89	105.08	2.12
	DF- DDM3Y1			16.7	0.556	1.1637	1885	349.69	105.08	1.51
	DF- CDM3Y6			16.7	0.556	1.191	1903	343.25	105.08	1.61
	DF- BDM3Y1			16.7	0.556	1.2225	1894	333.91	105.08	1.24
104	OM	93.25	0.731	17.25	0.541		1873	356.07	107.74	3.24
	DF- CDM3Y1			17.25	0.541	1.1157	1823	343.9	107.74	2.82
	DF- DDM3Y1			17.25	0.541	1. 1717	1829	327.82	107.74	2.2
	DF- CDM3Y6			17.25	0.541	1. 2687	1832	304.59	107.74	2.19
	DF- BDM3Y1			17.25	0.541	1.3312	1837	290.02	107.74	1.79

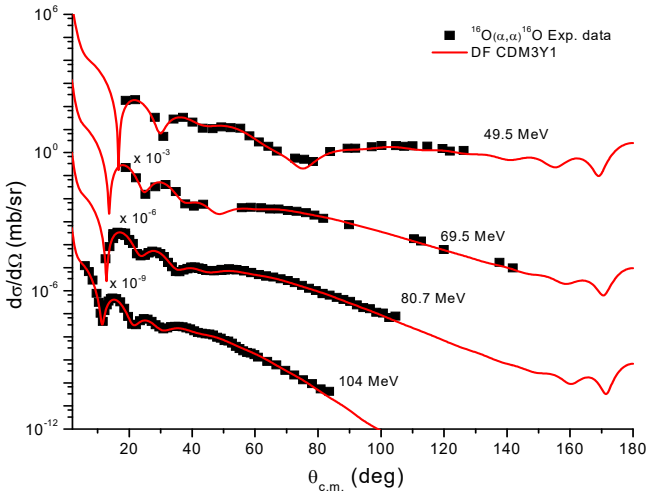

Fig. 13 The comparison between the experimental data for α+^{16}O at energies (49.5, 69.5, 80.7 and 104 MeV) and the theoretical calculations using DFP of interaction model CDM3Y1

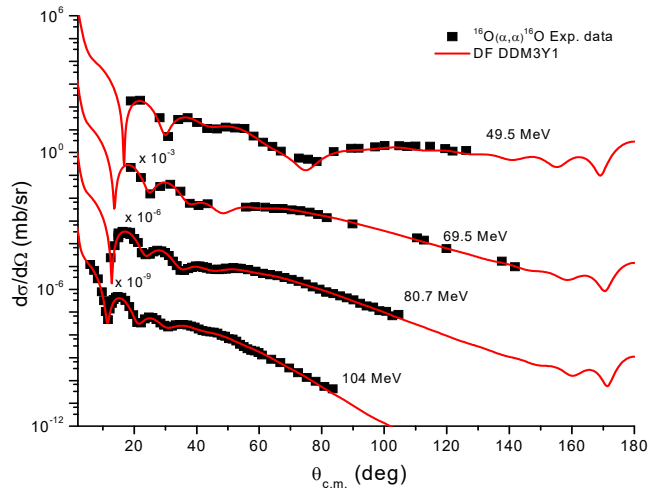

Fig. 14 The same as Fig. 13 but for interaction model DDM3Y1

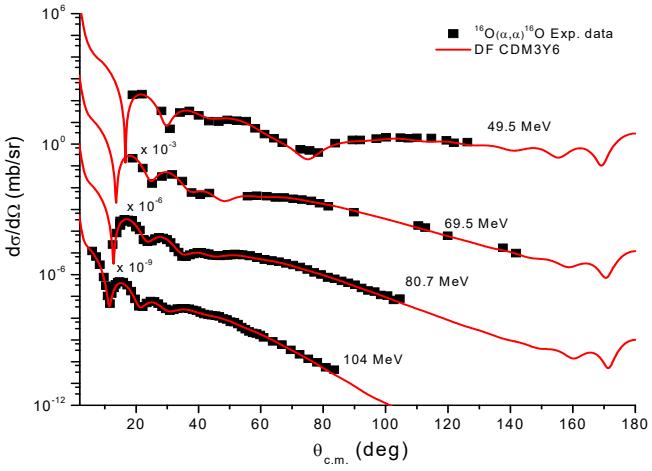

Fig. 15 The same as Fig. 13 but for interaction model CDM3Y6

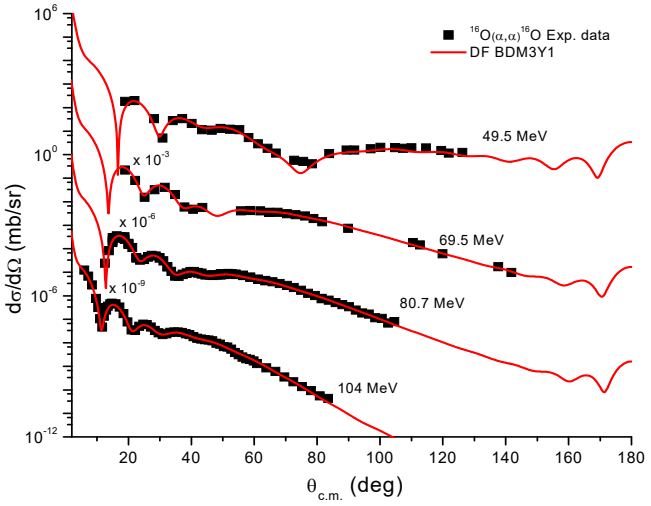

Fig. 16 The same as Fig. 13 but for interaction model BDM3Y1

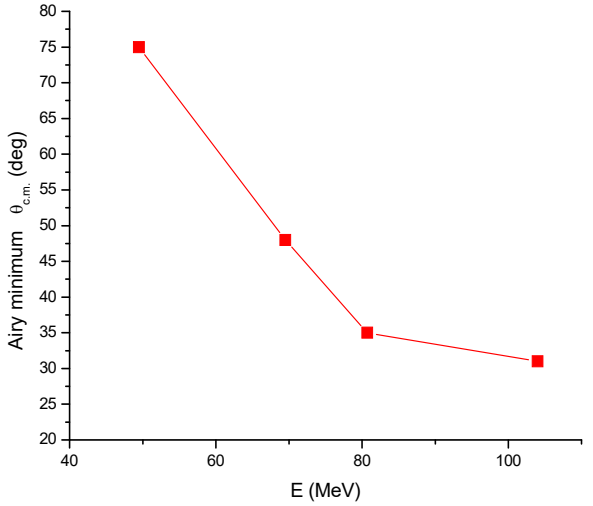

Fig. 17 Angular position of the Airy minimum for α+^{16}O elastic scattering at energies 49.5, 69.5, 80.7 and 104 MeV. The lines are only to guide the eye

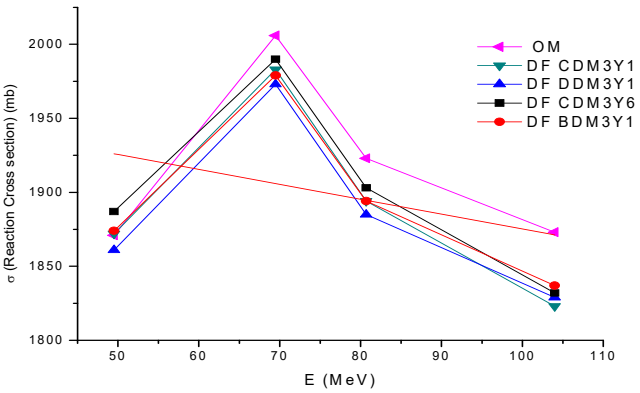

Fig. 18 The variation of reaction cross section with energy

We have calculated the reaction cross section (σ_R) at the different concerned energies using both OM and DF of different interaction models as shown in Fig. 18. The energy

dependence of reaction cross section can be expressed as $\sigma = 1854 - 2.128\,E$.

The J_v values from both OP and DFP in our work ranged between 290.02 and 382.18 MeV.fm^3 and decreased with increasing energy while the J_w ranges between 62.22 and 107.74 MeV.fm^3 and increases with increasing energy as shown in Table III which agree well with the previously existing theoretical estimations [18], [19]. The energy dependence of real volume integral in this work could be expressed as J_v = 399.15-0.354E, and for imaginary volume integral J_w = 34.68+0.787E as shown in Fig. 19.

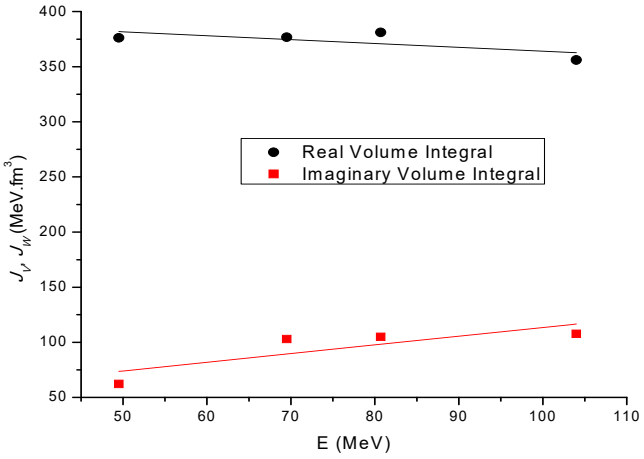

Fig. 19 Energy dependence of real (J_v) and imaginary (J_w) volume integral

The dependence of V_0 (depth for the real volume part of potential) and W_0 (depth for the imaginary volume part of potential) for ^{16}O(α, α)^{16}O nuclear system on energy are shown in Figs. 20 (a) and (b) and can be approximated by

(a) V = 122.47-0.28E,

(b) W = 3.468+0.146E.

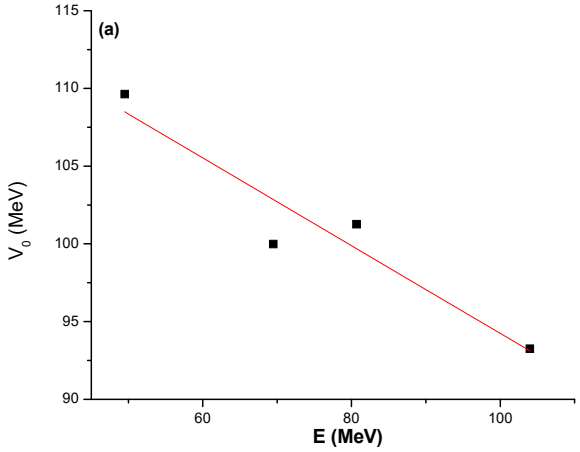

Fig. 20 (a) Energy dependence of real potential depth

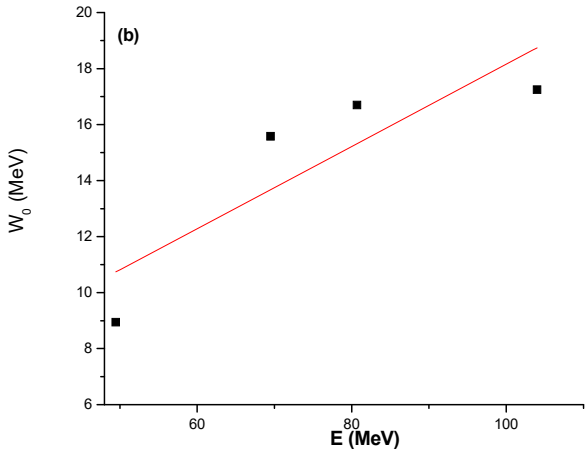

Fig. 20 (b) Energy dependence of imaginary potential depth

Fig. 21 shows the variation of the potential depth with radius for the direct and exchange parts of the potential and also their sum (Direct + Exchange) for α+^{16}O nuclear system at E_α=49.5 MeV using DF-CDM3Y1. Fig. 22 shows that the potential created by BDM3Y1 model of interaction has the shallowest depth in comparison with the rest, which reflects the necessity to use higher renormalization factor.

IV. Summary

We reanalyzed the available experimental angular distribution data for (α+^{12}C and α+^{16}O) nuclear systems using both OP and DFP of different interaction models. Refractive features and nuclear rainbow phenomenon is presented and well reproduced by theoretical calculations. Analysis of experimental data using DFP of different interaction models: CDM3Y1, CDM3Y6, DDM3Y1 and BDM3Y1 showed that, the potential created by BDM3Y1 model of interaction has the shallowest depth which reflects the necessity to use higher renormalization factor, and the potential created by CDM3Y1 model of interaction is the deepest which reflects the necessity to use smaller renormalization factor. Both (OP) and (DFP) of different interaction models reasonably reproduce the experimental data. The obtained N_r using all the aforementioned interaction models for α+^{12}C nuclear system is in the range 1.041 – 1.238. For α+^{16}O, N_r is in the range 1.1157 – 1.3312. Theoretical calculations showed that DF-CDM3Y1 is the most preferable interaction model in analysis α+^{12}C and α+^{16}O nuclear systems as it gives us the closest values of N_r to unity.

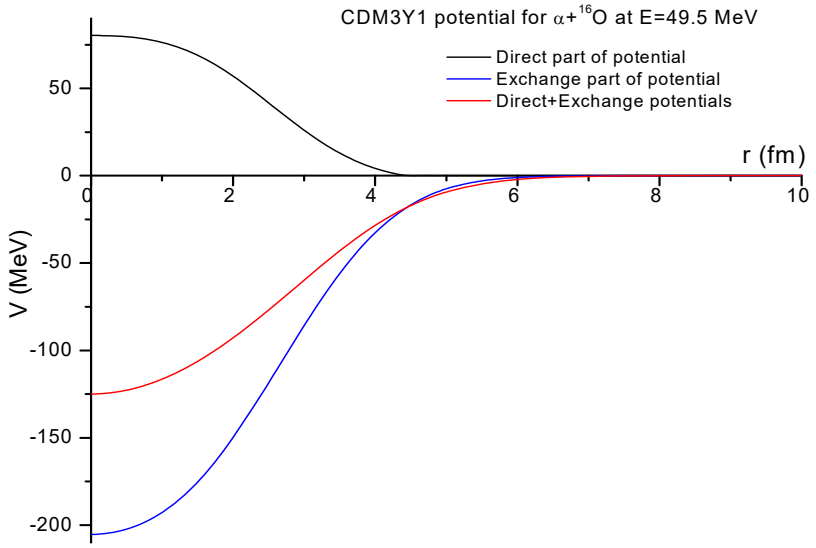

Fig. 21 The variation of the potential depth with radius for both Direct and Exchange parts of the potential and also their sum (Direct + Exchange) at E_α=49.5 MeV

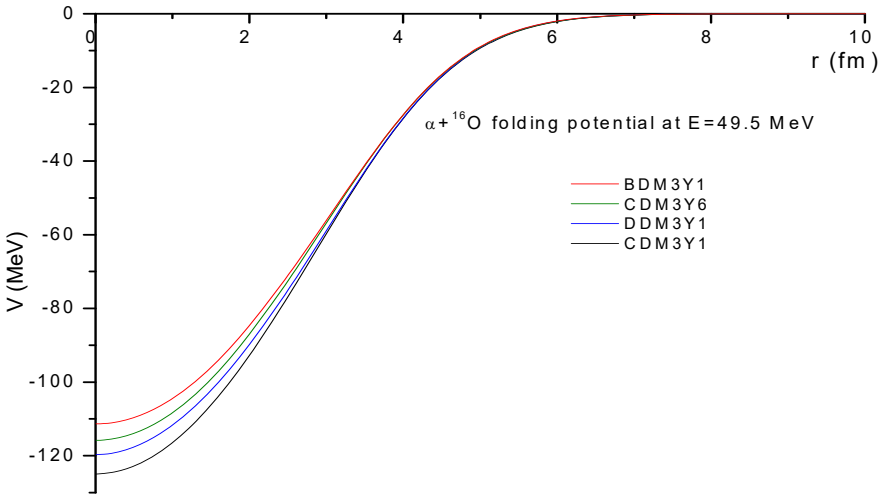

Fig. 22 The variation of the potential depth with radius for α+^{16}O folding potential at E_α =49.5 MeV using different interaction models: CDM3Y1, DDM3Y1, CDM3Y6 and BDM3Y1

REFERENCES

[1] D. A. Goldberg, S. M. Smith and G. F. Burdzik, Phys. Rev. C 10 (1974) 1362.
[2] R. M. DeVries, D. A. Goldberg, J. W. Watson, M. S. Zisman, and J. G. Cramer, Phys. Rev. Lett. 39 (1977) 450.
[3] P. Schwandt, S. Kailas, W. W. Jacobs, M. D. Kaitchuck, W. Ploughe, and P. P. Singh, Phys. Rev. C 21 (1980) 1656.
[4] A. A. Ogloblin, Yu. A. Glukhov, W. H. Trzaska, A. S. Dem'yanova, S. A. Goncharov, R. Julin, S. V. Klebnikov, M. Mutterer, M. V. Rozhkov, V. P. Rudakov, G. P. Tiorin, Dao T. Khoa, and G. R. Satchler, Phys. Rev. C 62 (2000) 044601.
[5] M. P. Nicoli, F. Haas, R. M. Freeman, S. Szilner, Z. Basrak, A. Morsad, G. R. Satchler, and M. E. Brandan, Phys. Rev. C 61 (2000) 034609.
[6] Yu. A. Glukhov, S. A. Goncharov, A. S. Dem'yanova, A. A. Ogloblin, M. V. Rozhkov, V. P. Rudakov, V. Trashka, J. IZV 65 (2001) 647.
[7] M. Buenerd, P. Martin, R. Bertholet, C. Guet, M. Maurel, J. Mougey, H. Nifenecker, J. Pinston, P. Perrin, F. Schussler, J. Jullen, J. P. Bondorf, L. Carlen, H. Å. Gustafsson, B. Jakobsson, T. Johansson, P. Kristiansson, O. B. Nielsen, A. Oskarsson, I. Otterlund, H. Ryde, B. Schröder, and G. Tibell, Phys. Rev. C 26 (1982) 1299.
[8] S. Kubono, K. Morita, M.H. Tanaka, M. Sugitani, H. Utsunomiya, H. Yonehara, M.-K. Tanaka, S. Shimoura, E. Takada, M. Fukuda, K. Takimoto, Phys. Lett. B. 127 (1983) 19.
[9] H. G. Bohlen, X. S. Chen, J. G. Cramer, P. Fröbrich, B. Gebauer, H. Lettau, A. Miczaika, W. von Oertzen, R. Ulrich, T. Wilpert, Z. Phys. A. 322 (1985) 241.
[10] A. J. Cole, W. D. M. Rae, M. E. Brandan, A. Dacal, B. G. Harvey, R. Legrain, M. J. Murphy, R. G. Stokstad, Phys. Rev. Lett. 47 (1981) 1705.
[11] M. Buenerd, A. Lounis, J. Chauvin, D. Lebrun, P. Martin, G. Duhamel, J.C. Gondrand, P. De Saintignon, Nucl. Phys. A. 424 (1984) 313.
[12] J.Y. Hostachy, M. Buenerd, J. Chauvin, D. Lebrun, Ph. Martin, B. Bonin, G. Bruge, J.C. Lugol, L. Papineau, P. Roussel, J. Arvieux, C. Cerruti, Phys. Lett. B. 184 (1987) 139.
[13] C.C. Sahm, T. Murakami, J.G. Cramer, A.J. Lazzarini, D.D. Leach, D.R. Tieger, R.A. Loveman, W.G. Lynch, M.B. Tsang, J. Van der, Phys. Rev. C 34 (1986) 2165.
[14] M. E. Brandan, Phys. Rev. Lett. 60 (1988) 784.
[15] M. El-Azab Farid, Z. M. M. Mahmoud, and G. S. Hassan, Phys. Rev. C 64 (2001) 014310.
[16] Dao T. Khoa, Phys. Rev. C 63 (2001) 034007.
[17] Sh. Hamada, Y. Hirabayashi, N. Burtebayev, S Ohkubo, Phys. Rev. C 87, 024311 (2013).

[18] Y. Hirabayashi and S. Ohkubo, Phys. Rev. C 88 014314 (2013).
[19] D. A. Goldberg and S. M. Smith, Phys. Rev. Lett. 33 (1974) 715.
[20] F. Michel, J. Albinski, P. Belery, Th. Delbar, Gh. Grégoire, B. Tasiaux, and G. Reidemeister, Phys. Rev. C 28(1983) 1904.
[21] H. Abele, H. J. Hauser, A. Körber, W. Leitner, R. Neu, H. Plappert, T. Rohwer, G. Staudt, M. Strasser, S. Weite, and M. Walz, Z. Phys. A 326, 373 (1987).
[22] F. Michel, Phys. Lett. 60B (1976) 229.
[23] Z. Majka, H. J. Gils, and H. Rebel, Phys. Rev. C 25 (1982) 2996.
[24] M. El-Azab Farid, J. Phys. G 16 (1990) 461.
[25] S. A. E. Khallaf, A. M. Amry, and S. R. Mokhtar, Phys. Rev.C 56 (1997) 2093.
[26] I. I. Gontchar and M. V. Chushnyakova, Comput. Phys. Commun. 181 (2010) 168.
[27] Dao T. Khoa, G.R. Satchler, W. von Oertzen, Phys. Rev. C 56 (1997) 954.
[28] S. Qing-biao, F. Da-chun and Z. Yi-Zhong, Phys. Rev. C 43(1991) 2773.
[29] G.R. Satchler, W.G. Love, Phys. Rep. 55 (1979) 183.
[30] I. J. Thompson, Comput. Phys. Rep. 7 (1988) 167.
[31] B. Tatischeff, I. Brissauud, Nucl. Phys. A. 155 (1970) 89.
[32] S. Wiktor, C. Mayer-Böricke, A. Kiss, M. Rogge, P. Turek, H. Dabrowski, Acta Phys. Pol. B 12 (1981) 491.
[33] G. Hauser, R. Löhken, H. Rebel, G. Schatz, G.W. Schweimer, J. Specht, Nucl. Phys. A. 128 (1969) 81.
[34] M. Yasue, T. Tanabe, F. Soga, J. Kokame, F. Shimokoshi, J. Kasagi, Y. Toba, Y. Kadota, T. Ohsawa, K. Furuno, Nucl. Phys. A. 394 (1983) 14.
[35] S. M. Smith, G. Tibell, A. A. Cowley, D. A. Goldberg, H. G. Pugh, W. Reichart, N.S. Wall, Nucl. Phys. A. 207 (1973) 273.
[36] M. Reed thesis, Lawrence Berkeley National Laboratory, Berkeley, CA, USA (1968).